8. G. A. Frolov, V. V. Pasichnyi, E. I. Suzdal'tsev, and V. S. Tsyganenko, Inzh.-Fiz. Zh., **57**, No. 2, 313-318 (1989).
9. G. A. Frolov, A. A. Korol. V. V. Pasichnyi et al., Inzh.-Fiz. Zh. **51**, No. 6, 932-940 (1986).
10. V. N. Eliseev and V. A. Solovov, Heliotekhnika, No. 6, 45-49 (1983).
11. A. M. Mikhalev and S. V. Reznik, Izv. Vyssh. Uchebn. Zaved., No. 4, 55-59 (1988).
12. R. E. Krzhizhanovskii and Z. Yu. Shteri, Thermophysical Properties of Nonmetallic Materials (Oxides) [in Russian], Leningrad (1973).

DETERMINATION OF QUASISTATIONARY MATERIAL SURFACE DESTRUCTION RATE FROM LINEAR ENTRAINMENT MEASUREMENTS IN THE NONSTATIONARY REGIME

G. A. Frolov, A. V. Bondarenko, V. V. Pasichnyi, and N. E. Aleksandrova

UDC 536.2.083

A method is proposed for determining the quasistationary linear entrainment rate $\bar{V}_\infty$ and the nonstationary entrainment parameter d_0 from measurements of the thickness of the entrained layer during the nonstationary period of the destruction of the surface of a material.

One of the most important characteristics of a heat-shielding material is the rate of destruction of its surface during interaction with a high-temperature medium [1]. It is especially important to determine the quasistationary entrainment rate $\bar{V}_\infty$, which it is necessary to know in order to calculate the effective enthalpy and to compare different materials with one another. Moreover, as shown in [2], the rate $\bar{V}_\infty$ must be achieved in order to determine the nonstationary entrainment parameter d_0, which in some cases makes it possible to calculate nonstationary mass entrainment without the use of high-temperature thermophysical characteristics.

During experiments it may happen that the apparatus does not operate long enough in order for a quasistationary rate $\bar{V}_\infty$ to be established. In this case the equations derived in [2] on the basis of the destruction constant K_{T_d} and the nonstationary entrainment parameter d_0

$$S(\tau) = \left(\frac{\sqrt{\tau} - \sqrt{\tau_{ent}}}{\sqrt{\tau_v} - \sqrt{\tau_{ent}}}\right)^2 S(\tau_v), \tag{1}$$

$$\tau_v = \frac{K_{T_d}}{1 - K_{T_d}} \frac{d_0}{\bar{V}_\infty} = 2{,}83 \frac{d_0}{\bar{V}_\infty}, \tag{2}$$

$$S(\tau_v) = \frac{2K_{T_d} - 1}{1 - K_{T_d}} d_0 = 1{,}83 d_0, \tag{3}$$

suggest a method for determining the quasistationary entrainment rate and the parameter d_0 itself.

Institute of Problems in Material Science, Academy of Sciences of Ukraine, Kiev. Translated from Inzhenerno-Fizicheskii Zhurnal, Vol. 62, No. 4, pp. 552-554, April, 1992. Original article submitted August 6, 1991.

 1062-0125/92/6204-0396$12.50

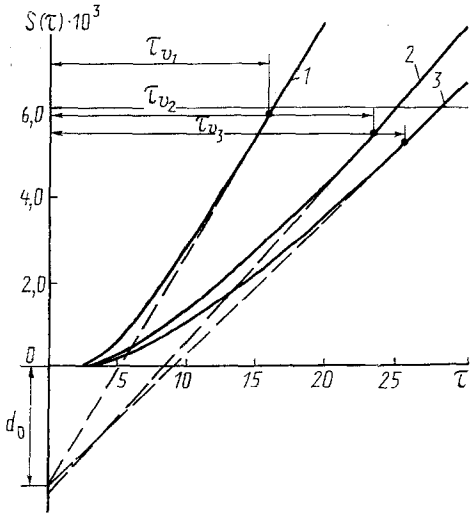

Fig. 1. Linear entrainment for quartz glass (λ = 10.4 W/(m·K)) as a function of the heating time with $P_e = 0.13 \cdot 10^5$ Pa. The curves were calculated according to the model described in [1]: 1) μ = exp[(68,800/T_w) − 24.59]; 2) μ = exp[(50,500/T_w) − 15.0]; 3) $\mu = 9.8 \times$ exp[(exp(1180/T_w + 10.05)/T_w) − 9.5] (kg·sec)m^2. $S(\tau)$, m; τ, sec.

In order to calculate the linear-entrainment parameters a functional of the following form is constructed:

$$F = \sum_{\tau=\tau_{ent}}^{\tau=\tau_v} [S(\tau)_{exp} - S(\tau)]^2, \tag{4}$$

where $S(\tau)$ is calculated using the formula (1) and depends on the time and three unknown parameters x_1, x_2, and x_3:

$$S(\tau, x) = \left\{\frac{\sqrt{\tau} - \sqrt{x_1}}{\sqrt{x_2} - \sqrt{x_1}}\right\}^2 x_3, \tag{5}$$

where $x - \tau_{ent}$; $x_2 - \tau_v$; $x_3 - S(\tau_v)$; $S(\tau)_{exp}$ is the array of experimental values of linear entrainment. The problem of optimizing the functional of the sum of the standard deviations

$$F = \sum_{\tau=\tau_{ent}}^{\tau=\tau_v} \left[S(\tau)_{exp} - \left\{\frac{\sqrt{\tau} - \sqrt{x_1}}{\sqrt{x_2} - \sqrt{x_1}}\right\}^2 x_3\right]^2 \to \min \tag{6}$$

in a restricted range of admissible values of x_1, x_2, x_3 ($a_i \le x_i \le b_i$) is solved by the method of modified random search using the coordinatewise self-teaching algorithm with a prescribed law of variation of probabilities [3]. The parameters a_i and b_i (i = 1-3) (the lower and upper limits of the variable x_i) are determined approximately from the expected values of x_i with the addition of some quantity Δ.

After entrainment at the end of the nonstationary period $S(\tau_v)$ and the time τ_v at which it is achieved are determined, the parameter d_0 and the entrainment rate $\bar{V}_\infty$ are found from the formulas (2) and (3).

The method was tested on the computed and experimental linear entrainment curves obtained in [1] (Fig. 1) and in [4, 5] (Fig. 2) for quartz glass. The results of the calculations, presented in Table 1, show that the values of the entrainment rate $\bar{V}_\infty$ and the parameter d_0 which are determined from the computed dependences $S(\tau)$ during the nonstationary period (for $\tau < \tau_v$) differ from those found in the quasistationary destruction regime by not more than 5-10%. These errors are doubled

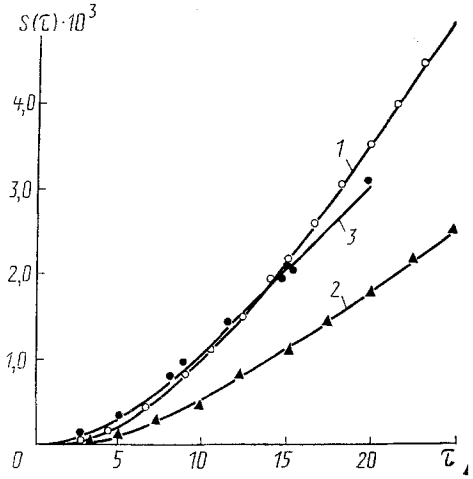

Fig. 2. Experimental curves of nonstationary linear entrainment for quartz glass; 1, 2) data of [4], 3) [5]; 1, 3) transparent and 2) opaque quartz glass (the test conditions are displayed in Table 1).

TABLE 1. Results of Determination of the Entrainment Rate $\bar{V}_\infty$ and the Parameter d_0 for Quartz Glass in the Nonstationary and Quasistationary Destruction Regimes (I – according to the stationary dependences $S(\tau)$; II – from nonstationary dependences with the help of the formulas (1)-(3)).

No.	Stagnation enthalpy and pressure		Computational results			$\bar{V}_\infty \cdot 10^3$, m/sec		$d_0 \cdot 10^3$, m	
	$P_e \cdot 10^5$, Pa	I_e, kJ/kg	τ_{ent}, s	τ_v, s	$S(\tau_v) \cdot 10^3$, m	I	II	I	II
1	0,13	20000	2,54	27,8	5,64	0,31	0,31	2,9	3,09
2	0,13	20000	2,51	22,6	5,16	0,37	0,35	3,1	2,83
3	0,13	20000	2,0	14,5	4,97	0,55	0,53	2,85	2,72
4	0,13	18820	2,88	27,5	5,8	0,31	0,33	2,8	3,18
5	0,13	18820	2,69	26,6	2,79	0,15	0,16	1,34	1,53
6	~1,0	8600	0,92	19,4	2,86	0,21	0,23	1,35	1,57

Note. 1, 3) computed regimes [1], distinguished by the value of the viscosity of quartz glass; 4, 5) experiment [4]; 6) experiment [5].

when the experimental curves of $S(\tau)$ are used in the cases considered.

NOTATION

τ, heating time; $\bar{V}_\infty$, quasistationary linear entrainment rate; $S(\tau)$ linear entrainment; $S(\tau_v)$ and τ_v, respectively, linear entrainment at the moment destruction rate becomes quasistationary and the time at which the linear entrainment is achieved; τ_{ent}, time of onset of destruction of the surface; K_{T_d}, destruction constant, determining the laws of variation of the surface temperature and the mass entrainment rate under conditions of nonstationary destruction of the surface of the material; d_0, nonstationary entrainment parameter, which depends weakly on the conditions of heating and all properties of the material, except of the thermal conductivity, and is numerically equal to the reduction of entrainment due to the presence of a nonstationary period of surface destruction.

LITERATURE CITED

1. Yu. V. Polezhaev and F. B. Yurevich, Heat Shields [in Russian], Moscow (1976).
2. Yu. V. Polezhaev and G. A. Frolov, Inzh.-Fiz. Zh., **56**, No. 4, 533-539 (1989).
3. D. Himmelblau, Applied Nonlinear Programming, McGraw-Hill, N.Y. (1972).
4. M. C. Adams, W. E. Powers, and S. J. Georgiev, J. Aero/Space Sci., **27**, No. 7, 535-547 (1960).
5. G. A. Frolov, V. V. Pasichnyi, Yu. V. Polezhaev, and A. V. Choba, Inzh.-Fiz. Zh., **52**, No. 1, 33-37 (1987).

THERMAL PROTECTION OF AN AREA FROM AN INCIDENT GAS JET

V. A. Vlasov and Yu. G. Zhulev

UDC 532.525.6

Results are offered from an experimental study of the decrease in thermal effect of a jet upon a normally oriented surface produced by introduction of cold air or water into the central portion of the jet.

As was shown in [1], one of the possible methods for reducing the effect of a hot gas jet on a normally oriented surface is to feed a coolant (cold air or water) from out of the surface in the vicinity of the critical point (Fig. 1a). In the present study we will consider a method for thermal effect reduction in which the jet itself includes a mechanism for thermal protection of the surface upon which it impinges. We will consider supply to the central portion of the jet of either cold air, cold water, or both (Fig. 1b). Both methods shown in Fig. 1 are intended to form a fan-shaped protective jet along the surface.

The arrangement of the experimental configuration is evident from Fig. 1b. A jet of hot air (having traversed an electrical heater) passes through a constricting nozzle and impinges on a barrier in the form of a thin stainless steel disk with back side coated by thermal insulation material. The cooling agent is fed through a coaxial tube located on the nozzle axis.

During the experiments the following quantities were measured: mass flow rate G, temperature T_0, and pressure P_0 of the hot air, mass flow rate G_c and temperature T_c of the cooling agent, and temperature distribution T_w over the disk, across the diameter of which thermocouples were installed symmetrically with respect to the center. The hot junctions of the thermocouples were soldered into copper cylinders (2.5 mm diameter) riveted into holes through the disk. The experimental results can be presented in the form of dimensionless wall temperature: $\theta = (T_w - T_c)/(T_0 - T_c)$, where the coolant (water or air) temperature is equal to the temperature of the surrounding medium, $T_c = T_i$.

The experiments were performed under the following conditions: nozzle diameter $D_n = 21$ mm, outer diameter of air and water supply tubes equal to $d_1 = 8$ mm and $d_2 = 3$ mm respectively (wall thickness 1 mm), relative distance from main nozzle mouth to disk $\bar{H} = 1.7$-6, relative distance from mouth of coaxial coolant supply tube to disk $\bar{h} = 0.15$ for coolant supply near the disk, or $\bar{h} = 1$ for coolant supply at nozzle mouth, hot air pressure reduction in nozzle $P_0/P_i = 1.7$-2.5, braking temperature in nozzle $T_0 = 590$-860 K, relative coolant flow rate $\bar{G}_{c\,max} = 1.4\%$ for water, and $\bar{G}_{c\,max} = 15\%$ for air.

The effectiveness of disk cooling for cooling air supply toward the critical point is evident from Fig. 2, which shows the functions $\theta = f(\bar{r}, \bar{G}_c, \bar{H}, \bar{h}, P_0/P_i, T_0)$. With increase in $\bar{G}_c$ the maximum disk temperature θ_{max} decreases, while its location moves away from the critical point. In particular, the following is evident: upon increase in P_0/P_i the quantity θ_{max}

Translated from Inzhenerno-Fizicheskii Zhurnal, Vol.62, No. 4, pp. 555-558, April, 1992. Original article submitted July 9, 1991.

1062-0125/92/6204-0398 $12.50